Optical and Recombination Losses in Cu 2 ZnSn(S,Se) 4 -Based Thin-Film Solar Cells with CdS, ZnSe, ZnS Window and ITO, ZnO Charge-Collecting Layers

Article *in* Journal of Nanoelectronics and Optoelectronics · February 2018

DOI: 10.1166/jno.2018.2192

CITATIONS
0

READS
57

4 authors, including:

Oleksandr A. Dobrozhan
Sumy State University
27 PUBLICATIONS **206** CITATIONS
SEE PROFILE

A. S. Opanasyuk
Sumy State University
132 PUBLICATIONS **439** CITATIONS
SEE PROFILE

Journal of
Nanoelectronics and Optoelectronics
Vol. 12, pp. 1–13, 2017
www.aspbs.com/jno

ARTICLE

Optical and Recombination Losses in $Cu_2ZnSn(S,Se)_4$-Based Thin-Film Solar Cells with CdS, ZnSe, ZnS Window and ITO, ZnO Charge-Collecting Layers

O. A. Dobrozhan*, P. S. Danylchenko, A. I. Novgorodtsev, and A. S. Opanasyuk

We report the investigation on the optical and recombination losses in the solar cells based on *n*-CdS(ZnSe, ZnS)/*p*-$Cu_2ZnSn(S,Se)_4$ heterojunctions with *n*-ITO(ZnO) frontal charge-collecting contacts. The calculation of the optical losses was carried out taking into account the light reflection from the interfaces of the contacted layers and absorption of the window and frontal charge-collecting layers. The recombination losses of the photogenerated charge carriers at the interface between the window and absorber layer, in the space charge and in the quasineutral regions of the semiconductor films was determined using the solution of the continuity equation. We investigated the effect of the optical and recombination losses on the internal (Q_{int}), external (Q_{ext}) quantum yields, short-circuit current density (J_{sc}) and maximum efficiency (η) of solar cells.

Keywords: $Cu_2ZnSn(S,Se)_4$ Solar Cells, Optical Losses, Recombination Losses, Quantum Yield, Short-Circuit Current, Efficiency.

1. INTRODUCTION

The future forecast for the renewable energy demonstrates that the solar power will become the dominant energy source from the middle of the 21st century.[1] One of the most perspective routes to utilize the solar energy is its conversion into electricity by using the solar cells (SCs). Even though silicon-based SCs are the most commercialized and widespread technology, thin-film SCs based on *n*-CdS/*p*-CdTe heterojunction (HJ) with *n*-ITO frontal charge-collecting contact have also been widely spread on the photovoltaic market.[2–4] However, the shortcomings, such as toxicity of Cd, high price and low abundance of In and Te, give rise to the search for the alternative materials to the functional layers in the photovoltaic devices. Nowadays, the compound $Cu_2ZnSn(S,Se)_4$ (CZTSSe) is regarded as a promising substitute for the traditional Si, CdTe, $Cu(In,Ga)(S,Se)_2$ absorber layers. CZTSSe possesses the controlled band gap for the solar light absorption ($E_g^{CZTSSe} = 1.0$–1.5 eV), *p*-type conductivity and high absorption coefficients ($\alpha \sim 10^4$–10^5 cm^{-1}).[5,6] The promising alternatives for the well-known SCs are considered the structure with ZnSe or ZnS window layers and ZnO charge collecting contact.[7–9] These structures contain only the abundant and non-toxic elements. ZnS, ZnO, ZnSe ($E_g^{ZnS} = 3.68$ eV, $E_g^{ZnO} = 3.37$ eV, $E_g^{ZnSe} = 2.67$ eV) are the wide-band gap semiconductors allowing to increase the number of the photons incoming to CZTSSe absorber layer.

According to Shockley-Queisser analysis, the maximum theoretical efficiency of the thin-film SCs with CZTSSe absorber layer is about (32–34)%.[5,10] However, the experimental efficiency of CZTSSe SCs is only 12.6%.[11,12] The difference between the theoretical and experimental values of the efficiency can be explained by the optical, electrical and recombination losses which take place during the conversion of the solar energy into electricity. The major irreversible losses of the energy during SC operation are associated with:

—reflection of the solar radiation both at the surface and HJs of SC;

Sumy State University, 2 Rymskogo-Korsakova st., 40007 Sumy, Ukraine
*Author to whom correspondence should be addressed.
Email: dobrozhan.a@gmail.com
Received: xx Xxxx xxxx
Accepted: xx Xxxx xxxx

—transmission of the solar radiation through SC without absorption;
—solar radiation absorption by the auxiliary layers of SC;
—scattering of the photon energy excess by the thermal lattice vibrations;
—recombination of the electron–hole pairs generated by the photon energy at the interfaces and in the bulk of absorber layer;
—internal series resistance;
—other physical processes.

The enhancement of the SC efficiency might be achieved by the minimization of the described losses by using the optimized structures based on the functional layers with the improved characteristics.

Up to now, the optical and recombination losses in the SCs based on *n*-CdS/*p*-Cu(In,Ga)Se_2,[13–15] *n*-CdS/*p*-CdTe,[13,16–25] *n*-ZnS/*p*-CdTe,[18,19,24] HJs and perovskite layers[26] were investigated. However, except the work,[27] there is a lack of research devoted to the study of such losses in the SCs based on CZTS absorber. Gorji et al. in Ref. [27] carried out the comparison of the SC efficiency for the following structures: FTO/CdS/CZTS, FTO/TiO_2/In_2S_3/CZTS and FTO/In_2S_3/CZTS. It was identified that the SC with 16% theoretical efficiency could be achieved by using TiO_2 as a charge-collecting contact and In_2S_3 as a window layer. The further evaluation of the effect of the recombination losses on the device efficiency was not performed. To the best of our knowledge, the attempts to apply ZnO as an alternative charge-collecting contact and ZnSe, ZnS as Cd-free window layers were not fully investigated. The foregoing discussions identified the main goal of this work—to determine and compare the optical and recombination losses in the SCs based on *n*-CdS(ZnSe, ZnS)/*p*-CZTSSe HJs with *n*-ITO(ZnO) frontal charge-collecting contacts.

2. THE CALCULATIONS OF THE OPTICAL LOSSES IN THE SCS DUE TO THE REFLECTION AND ABSORPTION OF SOLAR RADIATION

2.1. The Optical Losses in the SCs Due to the Reflection of Solar Radiation

In this work, the thin film SCs with a multilayer structure composed of the absorber (CZTSSe), window (CdS, ZnSe, ZnS) layers, charge-collecting contacts (ITO, ZnO) were examined. The light flow, before reaching CZTSSe absorber layer in which the generation of the electron–hole pairs is occurred, passes through the ITO(ZnO) and CdS(ZnSe, ZnS) layers of the SCs. Herewith, the optical losses of energy as a consequence of the light reflection from the air/ITO(ZnO), ITO(ZnO)/CdS(ZnSe, ZnS), CdS(ZnSe, ZnS)/CZTSSe interfaces and the light absorption of ITO(ZnO), CdS(ZnSe, ZnS) are observed.

The reflection coefficients at the interfaces of the contacted layers can be determined by using Fresnel equation:[20,28]

$$R = \left(\frac{n_i - n_j}{n_i + n_j}\right)^2 \quad (1)$$

where n_i, n_j—refractive indices of the first and second contacted materials, respectively.

In the case of the electrically conductive material, the reflection coefficients might be calculated by using the following expression:[14,24]

$$R_{ij} = \frac{|n_i^* - n_j^*|}{|n_i^* + n_j^*|} = \frac{(n_i - n_j)^2 + (k_i - k_j)^2}{(n_i + n_j)^2 + (k_i + k_j)^2} \quad (2)$$

where n_i^*, n_j^*—the complex refractive indices; k_i, k_j—the extinction coefficients.

The spectral dependencies of the refractive indices and extinction coefficients for each considered layer are shown in Figure 1.

The spectral dependencies of n and k were taken from the literature data on the refractive and extinction coefficients of ITO, ZnO, CdS, ZnSe, ZnS, CZTS.[5,29–31] It was assumed that the air has $n = 1$ and $k = 0$. The calculated spectral dependencies of the reflection coefficients of the SC layers in direct contact with air are shown in Figure 2.

The results showed that the lowest values of the reflection coefficients were observed at the interfaces between air and ZnO, $R = (0.12–0.14)$ at $\lambda \leq 350$ nm, and between air and ITO, $R = (0.01–0.10)$ at $\lambda = (350–1250)$ nm. The lowest values of $R = (0.15–0.21)$ among the investigated window layers were obtained at air/ZnS interface in the wavelength range of (350–1250) nm. The values of R for the interfaces air/CZTS were (0.22–0.27). The calculated spectral dependencies of the reflection coefficients for pairs of the contacted layers in the SCs are shown in Figure 3.

The values of the reflection coefficients of ZnO/(window layer) interface were lowest for ZnO/ZnS pair (Fig. 3(a)), $R = (0.002–0.007)$ at $\lambda = (385–1250)$ nm, but still, ZnO/CdS pair shows better values at $\lambda < 385$ nm. In the case of ITO/(window layer) interface (Fig. 3(b)), the lowest values of R (0.008–0.100) were demonstrated by ITO/ZnS in the almost overall spectral range (except a small interval in UV region). At the same time, these values were higher than those for ZnO/ZnS contact. In general, the values of R of the contacted layers are low due to the small difference between the optical constants of the materials. For comparison, the calculation results of the reflection from the interfaces in contact with air gave us much higher values (Fig. 2). Moreover, the reflection coefficients were low for the interfaces between CZTS absorber layer and window materials, such as CdS, ZnSe, ZnS (Fig. 3(c)). It indicates that all investigated layers, having the low reflection coefficients, are perspective

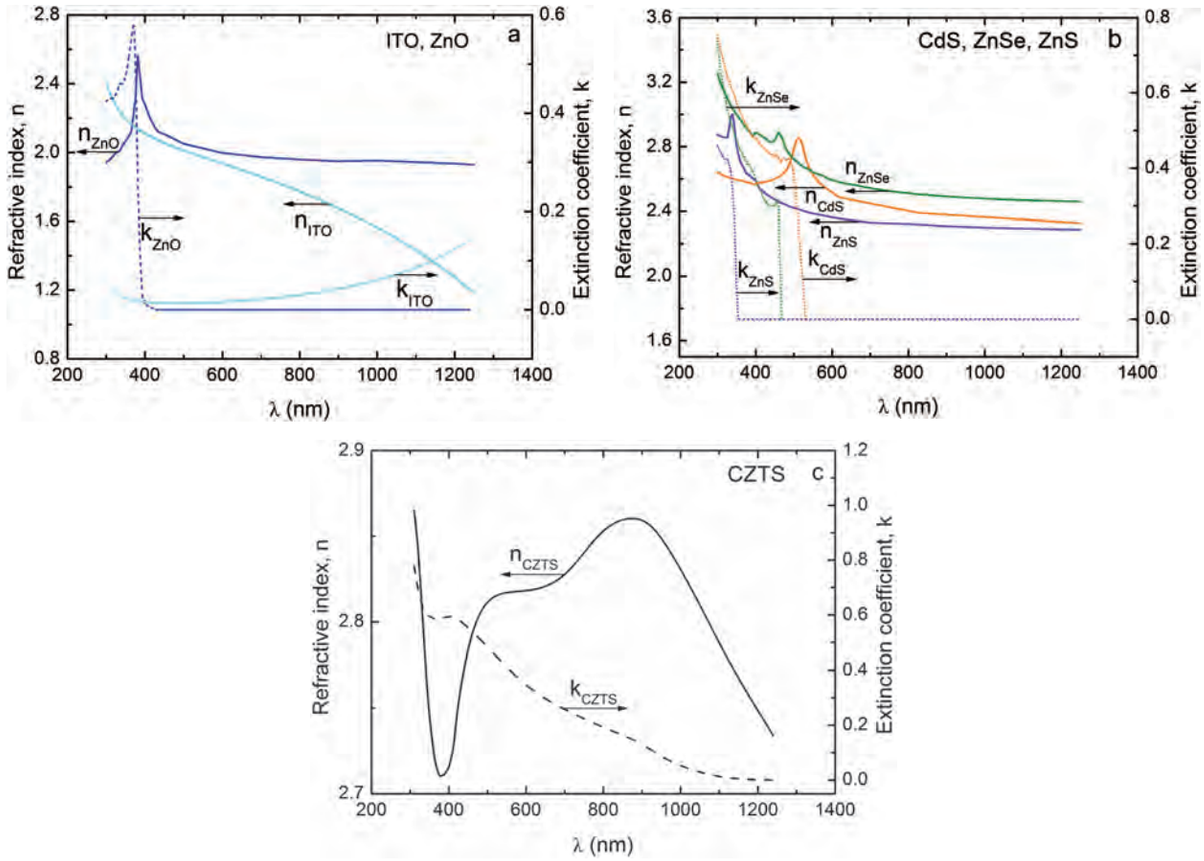

Fig. 1. Spectral dependencies of the refractive indices (n) and extinction coefficients (k) of (ITO, ZnO) (a), (CdS, ZnSe, ZnS) (b) and CZTS (c).

for the SCs design. Nonetheless, as can be seen from Figure 3(c), ZnSe layer provided the minimum reflection coefficients, $R = (0.003–0.007)$, at the window-absorber interface in the wavelength range of $\lambda = (540–1250)$ nm and CdS layer at $\lambda < 540$ nm. Noteworthy, as indicated in Ref. [31], zinc selenide possesses junction close to the ideal with CZTS due to the good agreement of the lattice constants.

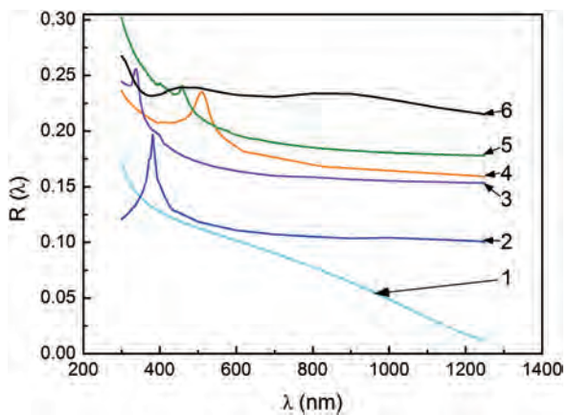

Fig. 2. Spectral dependencies of the reflection coefficients (R) at the interfaces: air/ITO (1), air/ZnO (2), air/ZnS (3), air/CdS (4), air/ZnSe (5) and air/CZTS (6).

In the case of the ignoring of the absorption processes, the transmission coefficients of the light through the auxiliary layers (ITO(ZnO), CdS(ZnSe, ZnS)) can be determined by the formula $T = 1 - R$. Thus, the transmission coefficients of the multilayer SC structure can be expressed as:[16, 20, 21]

$$T(\lambda) = (1 - R_{12})(1 - R_{23})(1 - R_{34}) \quad (3)$$

where R_{12}, R_{23}, R_{34}—the reflection coefficients from the interfaces: air/ITO(ZnO), ITO(ZnO)/CdS(ZnSe, ZnS), CdS(ZnSe, ZnS)/CZTS.

Noteworthy, the Eq. (3) does not account the multiple light reflections from the layers (ITO(ZnO), CdS(ZnSe, ZnS)), which is acceptable in the case of the low reflection coefficients at the material interfaces (Fig. 3). Besides, the low reflection coefficients allow to ignore the interference effects in the thin films. The calculation results of the spectral dependencies of the transmission coefficients in the SCs based on n-CdS(ZnSe, ZnS)/p-CZTS HJs with ITO and ZnO frontal contacts are presented in Figure 4.

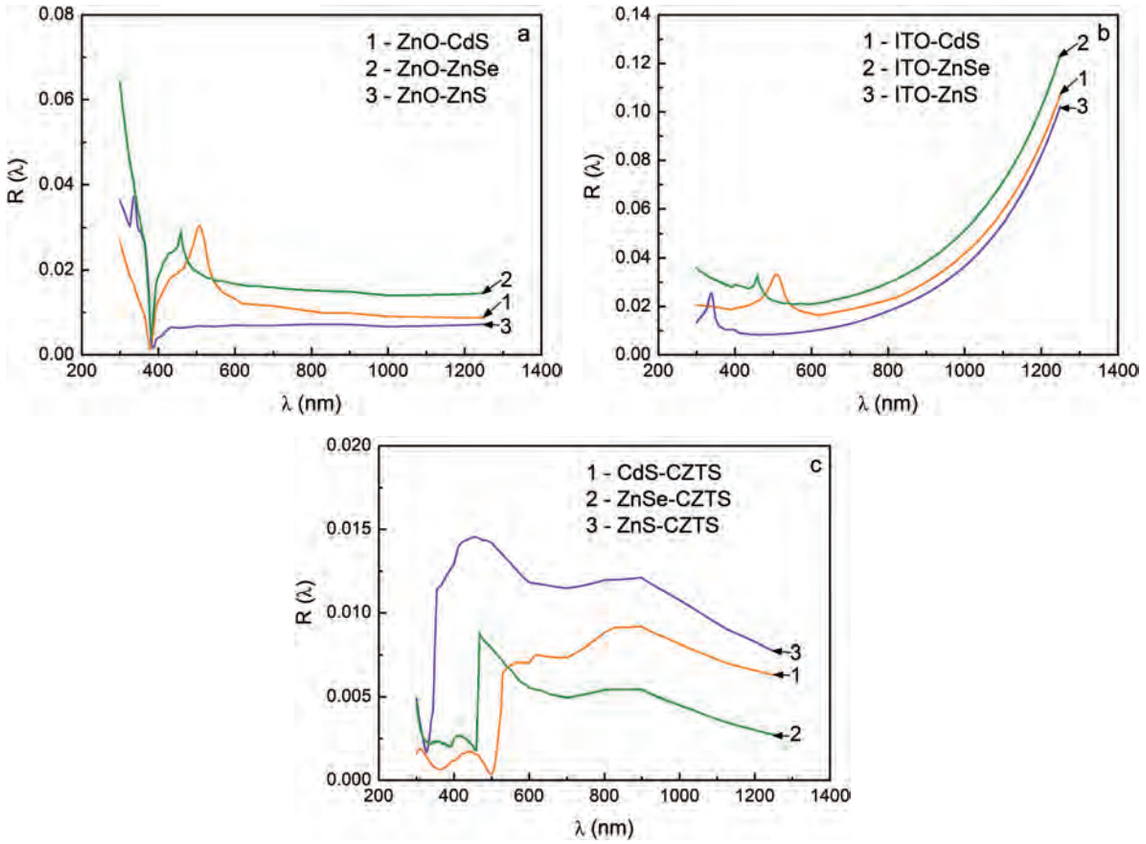

Fig. 3. Spectral dependencies of the reflection coefficients (R) of the contacted interfaces of the SCs: ZnO/(window layer) (a), ITO/(window layer) (b), (window layer)/CZTS (c).

Unfortunately, it is difficult to determine the optimal combination of the auxiliary layers of the SCs from Figure 4. For this purpose, we calculated the coefficients of the optical losses (Δ):

$$\Delta = \frac{T_{\max}(\lambda) - (1/n)\sum_{i=1}^{n} T_i(\lambda)}{T_{\max}(\lambda)} \quad (4)$$

Since $T_{\max} = 1$, the Eq. (4) can be simplified to the following one:

$$\Delta = 1 - \frac{1}{n}\sum_{i=1}^{n} T_i(\lambda) \quad (5)$$

The calculated coefficients of the optical losses for each investigated SC structure are presented in Table I.

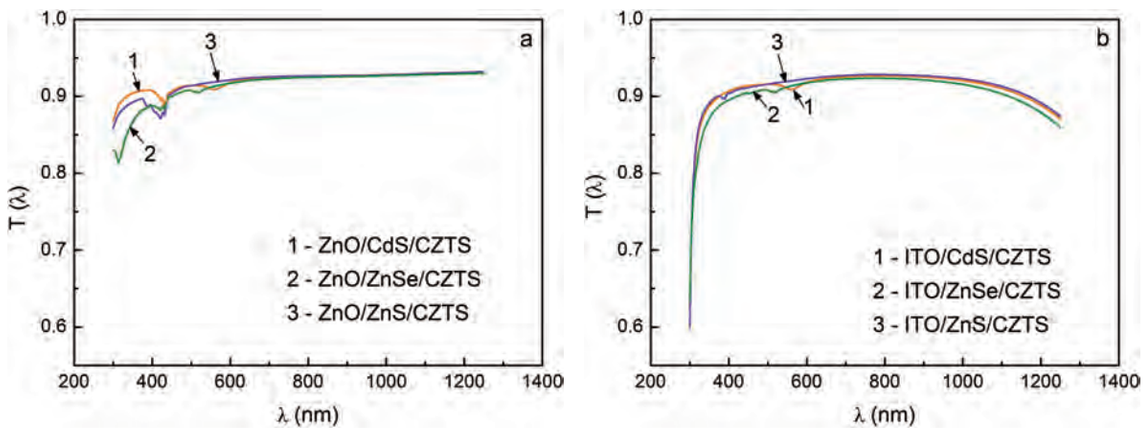

Fig. 4. Spectral dependencies of the transmission coefficients of the SCs with the structures ZnO/(window layer)/CZTS (a) and ITO/(window layer)/CZTS (b) taking into account the light reflection from the interfaces.

Table I. The coefficients of the optical losses (Δ) in the SCs with the different structures.

No.	Thin film SC structure	Loss coefficients, Δ (%)	Light transmission coefficients, T (%)
1	ZnO/CdS/CZTS	7.7	92.3
2	ZnO/ZnS/CZTS	7.8	92.2
3	ZnO/ZnSe/CZTS	8.1	91.9
4	ITO/ZnS/CZTS	8.6	91.4
5	ITO/CdS/CZTS	8.8	91.2
6	ITO/ZnSe/CZTS	9.4	90.6

As can be seen, the minimum optical losses were showed by SC with ZnO/CdS/CZTS structure ($T = 92.3\%$), and maximum optical losses—by ITO/ZnSe/CZTS structure ($T = 90.6\%$). The traditional SC with ITO, CdS layers demonstrated the high light transmission rate before reaching CZTS absorber layer (91.2%). The difference of the light losses in the auxiliary layers of SCs between the best (7.7%) and worst (9.4%) structures was not exceeded 1.7%. Hence, the optimization of SC structures should be carried out by the evaluation of other parameters, such as optical losses due to the light absorption of the auxiliary layers, recombination of free carriers, and quality of crystal lattice coupling in the materials.

2.2. The Optical Losses in the SCs Due to the Light Absorption

In general case, in addition to the reflection losses, we must consider the light absorption losses in the auxiliary layers of SCs. The transmission coefficients taking into account both the light reflection and absorption of the charge-collecting and window layers can be calculated using the expression:[16, 20, 21]

$$T(\lambda) = (1 - R_{12})(1 - R_{23})(1 - R_{34})(1 - R_{45}) \times \exp(-\alpha_1 d_1)\exp(-\alpha_2 d_2) \quad (6)$$

where α_1, α_2—the absorption coefficients of the charge-collecting and window layers; d_1, d_2—the charge-collecting and window layer thicknesses.

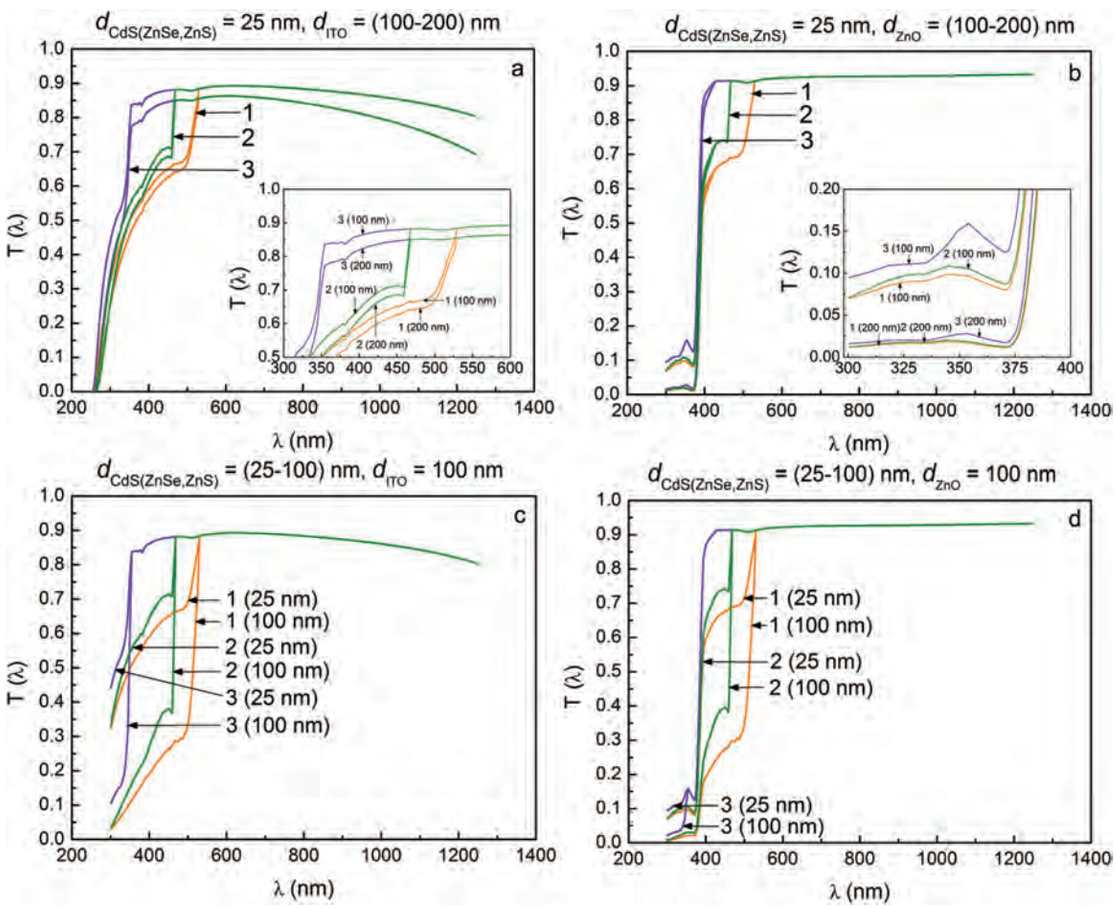

Fig. 5. Spectral dependencies of the transmission coefficients of the SCs with the structures ITO/CdS/CZTS (1), ITO/ZnSe/CZTS (2), ITO/ZnS/CZTS (3) (a, c); ZnO/CdS/CZTS (1), ZnO/ZnSe/CZTS (2), ZnO/ZnS/CZTS (3) (b, d) with the different thicknesses of the window and charge-collecting layers. The light reflection from the interfaces and absorption of the auxiliary layers were taken into account.

The absorption coefficients of the materials $\alpha(\lambda)$, considering the extinction coefficient $k(\lambda)$, can be calculated by using the following equation:[20, 21]

$$\alpha(\lambda) = \frac{4\pi}{\lambda}k \tag{7}$$

The modeling of the light reflection and absorption processes in the multilayer structures was carried out by using the different thicknesses of the window, $d_{\mathrm{CdS(ZnSe,\,ZnS)}} =$ (25–100) nm, and frontal charge-collecting, $d_{\mathrm{ITO(ZnO)}} =$ (100–200) nm, layers. These thickness values of the layers are typical for the practical SCs.

The spectral dependencies of the transmission coefficients of the SCs with ITO(ZnO), CdS(ZnSe, ZnS) layers, considering the absorption of the auxiliary layers with the different thicknesses, are depicted in Figure 5.

The calculated coefficients of the optical losses for each considered SC structure with different thicknesses of the window (CdS, ZnSe, ZnS) and charge-collecting (ITO, ZnO) layers are presented in Table II.

As it was expected, the replacement of the traditional window material (CdS) with wide band gap materials (ZnSe, ZnS) led to the increase in the transmission coefficients of the multilayer structures, primarily, in the short wave region at $d_{\mathrm{CdS(ZnSe,\,ZnS)}} =$ (25–100) nm. This tendency was valid for applying ITO and ZnO layers as the charge-collecting contacts with $d_{\mathrm{ITO(ZnO)}} =$ (100–200) nm.

ZnO layer is more attractive than ITO because it improves the light transmission coefficients toward CZTS absorber layer regardless of the considered window materials. As it was predicted, the increase of the thicknesses of the charge-collecting contact resulted in the deterioration of the transmission coefficients, and, as a consequence, to the decrease of SCs efficiencies. The similar effect was observed during the increasing of the thicknesses of the window layers. Thus, these auxiliary layers of the SCs should have the minimum technologically achievable thicknesses.

The analysis of the results presented in Figure 5 and Table II shows that the most appealing SC structure at the investigated thicknesses was ZnO/ZnS/CZTS. The worst structure in terms of the optical losses in the auxiliary layers was the traditional ITO/CdS/CZTS SC. It can be explained by the inferior characteristics of CdS window layer in the short wave region of the solar spectrum. The SCs containing ZnSe window layer exhibited the intermediate behavior between these structures. However, it should be noted that the values of T for the best and worst structures differed only in (5.2–13.5)%.

Table II. The coefficients of the optical losses in the SCs with the different structures (considering the light absorption of the auxiliary layers).

No.	Thin film solar cell structure	Loss coefficient, Δ (%)			
	$d_{\mathrm{ITO(ZnO)}} = 100$ nm				
	$d_{\mathrm{CdS(ZnSe,\,ZnS)}}$, nm	25	50	75	100
1	ZnO/ZnS/CZTS	14.8	15.0	15.1	15.2
2	ITO/ZnS/CZTS	15.0	15.9	16.5	16.9
3	ZnO/ZnSe/CZTS	16.7	18.3	19.5	20.4
4	ITO/ZnSe/CZTS	18.0	21.0	22.9	24.3
5	ZnO/CdS/CZTS	18.5	21.2	23.2	24.7
6	ITO/CdS/CZTS	20.0	24.1	26.9	28.7
	$d_{\mathrm{ITO(ZnO)}} = 200$ nm				
1	ZnO/ZnS/CZTS	16.1	16.4	16.7	17.0
2	ZnO/ZnSe/CZTS	17.6	18.9	19.9	20.7
3	ZnO/CdS/CZTS	19.3	21.7	23.5	24.9
4	ITO/ZnS/CZTS	20.4	21.1	21.6	22.0
5	ITO/ZnSe/CZTS	23.2	25.8	27.7	29.0
6	ITO/CdS/CZTS	25.0	27.4	27.5	27.5

3. THE DETERMINATION OF THE RECOMBINATION LOSSES IN THE SCS

3.1. The Width of the Space Charge Region (SCR) and Quantum Yield of the SCs

The important parameter for the determination of the SC efficiency is the internal quantum yield (Q_{int}). It is equal to the ratio between the photogenerated electron–hole pairs and the total amount of the photons, reached the absorber layer and created the drift (Q_{drift}) and diffusion (Q_{dif}) components of the photocurrent (J_{ph}). The internal quantum yield (Q_{int}) of the SC depends on the recombination losses, taking place at the interface of n-CdS(ZnSe, ZnS)/p-CZTS HJs, in the space charge and quasineutral regions of the heteropairs, and on the back surface of CZTS layer. Due to the optical losses owing to the light reflection and absorption of the auxiliary layers, the determination of the external quantum yields (Q_{ext}) is crucial for the evaluation of the device performance.[33, 34]

The important parameter for the analysis of the recombination losses in the SCs is the width of space charge region (w), in other words, the depletion region, occurring at the interface between the heteropairs, where the electrical field is acting as a separator for the photogenerated electron–hole pairs. This width mainly depends on the concentration of uncompensated acceptors ($N_a - N_d$) (i.e., the difference between the acceptor and donor concentrations), locating in the semiconductor materials, and the contact barrier height. However, the latter value for

Table III. The physical parameters of the materials used for the construction of the energy band diagrams and calculation of the contact barrier height at the HJs.[5, 30, 35–38, 39–41]

Parameter	n-CdS	n-ZnSe	n-ZnS	p-CZTS
Bang gap E_g, eV	2.42	2.67	3.68	1.13
Electron affinity χ, eV	4.50	4.09	3.90	4.30
Fermi level position E_F, eV	0.04	0.10	0.22	0.04
Electron work function W, eV	4.54	4.19	4.12	5.26
Permittivity ε	10.20	8.60	8.30	11.20
N_A, cm^{-3}	–	–	–	10^{18}
N_D, cm^{-3}	10^{17}	10^{16}	10^{16}	–

Table IV. Some calculated parameters of *n*-CdS(ZnSe, ZnS)/*p*-CZTS HJs.

Parameter (eV)	*n*-CdS/*p*-CZTS	*n*-ZnSe/*p*-CZTS	*n*-ZnS/*p*-CZTS
ΔE_c	0.20	−0.21	−0.40
ΔE_v	1.22	1.46	2.28
V_D	0.72	1.07	1.14
V_{CZTS}	0.01	0.08	0.34
V_{CdS}	0.71	–	–
V_{ZnS}	–	–	0.80
V_{ZnSe}	–	0.99	–

Table V. The values used for the calculation of w and Q.[5, 30, 38, 48–51]

Parameter	Value
$V_D - qU$, eV	$(0.72)_{CdS}$, $(1.07)_{ZnSe}$, $(1.14)_{ZnS}$
S, S_b, cm/s	10^7
τ_{np}, ns	7.8
τ_{pn}, ns	$(10)_{CdS}$, $(2)_{ZnSe}$, $(10)_{ZnS}$
D_{np}, cm^2/s	25
D_{nn}, cm^2/s	$(5)_{CdS}$, $(7)_{ZnSe}$, $(6)_{ZnS}$
D_{pp}, cm^2/s	2
T, K	300

the investigated junctions, unfortunately, was not known. This problem was solved by means of the construction of the energy band diagrams of the HJs. The important constants, used for the construction, are presented in Table III. It was considered that the small amount of the surface states exists at the interface between heteropairs. At the same time, the charge transport mechanism was described accordingly to Anderson model.

Then, the gaps between conduction (ΔE_c) and valence (ΔE_v) bands in the materials of *n*-CdS(ZnSe, ZnS)/*p*-CZTS HJs were determined using the equations presented in Refs. [42, 43].

It was assumed, that Fermi level positions in the contacted materials coincide with the formation energies of the intrinsic point defects.[35, 39, 41, 44] The calculated values of ΔE_c, ΔE_v, V_D, V_{CZTS}, $V_{CdS,\,ZnSe,\,ZnS}$ are presented in Table IV. By using these values, we constructed the energy band diagrams of the ideal *n*-CdS(ZnSe, ZnS)/*p*-CZTS HJs (energy band diagram of *n*-ZnS/*p*-CZTS is shown in Fig. 6). The values, used for the calculations of w and Q, are presented in Tables III–V.

Unlike the fact that the charge transport processes at *n*-CdS/*p*-CdTe HJ are analogous to those occurring in the Schottky diodes,[2] the same charge transport mechanisms for *n*-CdS(ZnSe, ZnS)/*p*-CZTS heterosystems are not acceptable. It is due to the fact that the doping levels in CZTS ($N_a = 10^{17}$–10^{18} cm^{-3}[45]) are higher than in CdTe material ($N_a = 10^{14}$–10^{17} cm^{-3}[34]) and even higher than in the window materials ($N_d = 10^{16}$–10^{17} cm^{-3}[30, 46]). It means that SCR is located both in the window (w_n) and absorber (w_p) layers, and SCR width can be determined by the equations:[47]

$$w_n = \sqrt{\frac{2\varepsilon_n\varepsilon_p\varepsilon_0 N_A(V_D - qU)}{q^2 N_D(N_A\varepsilon_p + N_D\varepsilon_n)}},$$
$$w_p = \sqrt{\frac{2\varepsilon_n\varepsilon_p\varepsilon_0 N_D(V_D - qU)}{q^2 N_A(N_A\varepsilon_n + N_D\varepsilon_p)}} \quad (8)$$
$$w = \sqrt{\frac{2\varepsilon_n\varepsilon_p\varepsilon_0(V_D - qU)}{q^2}\left(\frac{1}{\varepsilon_n N_D} + \frac{1}{\varepsilon_p N_A}\right)}$$

where ε_n, ε_p—the relative permittivity of the window and absorber materials; ε_0—the vacuum permittivity; $V_D = qV_{bi}$—the contact barrier height (V_{bi}—the built-in potential); U—the applied external voltage; q—the elementary charge; N_A, N_D—the concentration of uncompensated acceptors and donors in the absorber and window layers.

Kosyachenko et al. showed that the solution of the continuity equation is effective for the determination of the drift component of the internal quantum yield (Q_{drift}) of the SC, while taking into account the recombination at the HJ interface and in SCR, by using the following equation:[33, 34]

$$Q_{\text{drift}\,p(n)} = \frac{1 + (S/D_{pp(nn)})(\alpha_{p(n)} + (2\cdot(V_D - qU))/w_{p(n)}\cdot kT)^{-1}}{1 + (S/D_{pp(nn)})((2\cdot(V_D - qU))/w_{p(n)}\cdot kT)^{-1}} - \frac{\exp(-\alpha_{p(n)}w_{p(n)})}{1 + \alpha_{p(n)}\cdot L_{np(pn)}} \quad (9)$$

where S —the recombination velocity of the charge carriers at the HJ interface and in SCR; $D_{pp(nn)}$—the diffusion coefficients of the holes (electrons) in the absorber (window) layers; $\alpha_{p(n)}$—the light absorption coefficients of the absorber (window) layer; k—the Boltzmann constant; T—the temperature; $L_{np(pn)}$—the diffusion length of the electrons (holes) in the absorber (window) layer ($L_{n(p)} = (\tau_{n(p)}\cdot D_{n(p)})^{1/2}$, where $\tau_{n(p)}$—the lifetime of the electrons (holes), $D_{n(p)}$—the diffusion coefficients of the electrons (holes) in the relevant layers).

It should be noted that the Eq. (9) does not consider the recombination in the quasineutral regions of the window and absorber materials and on the back surface of CZTS

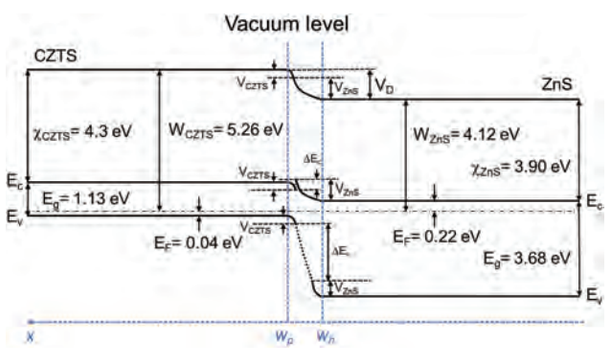

Fig. 6. Energy band diagrams of *n*-ZnS/*p*-CZTS HJ.

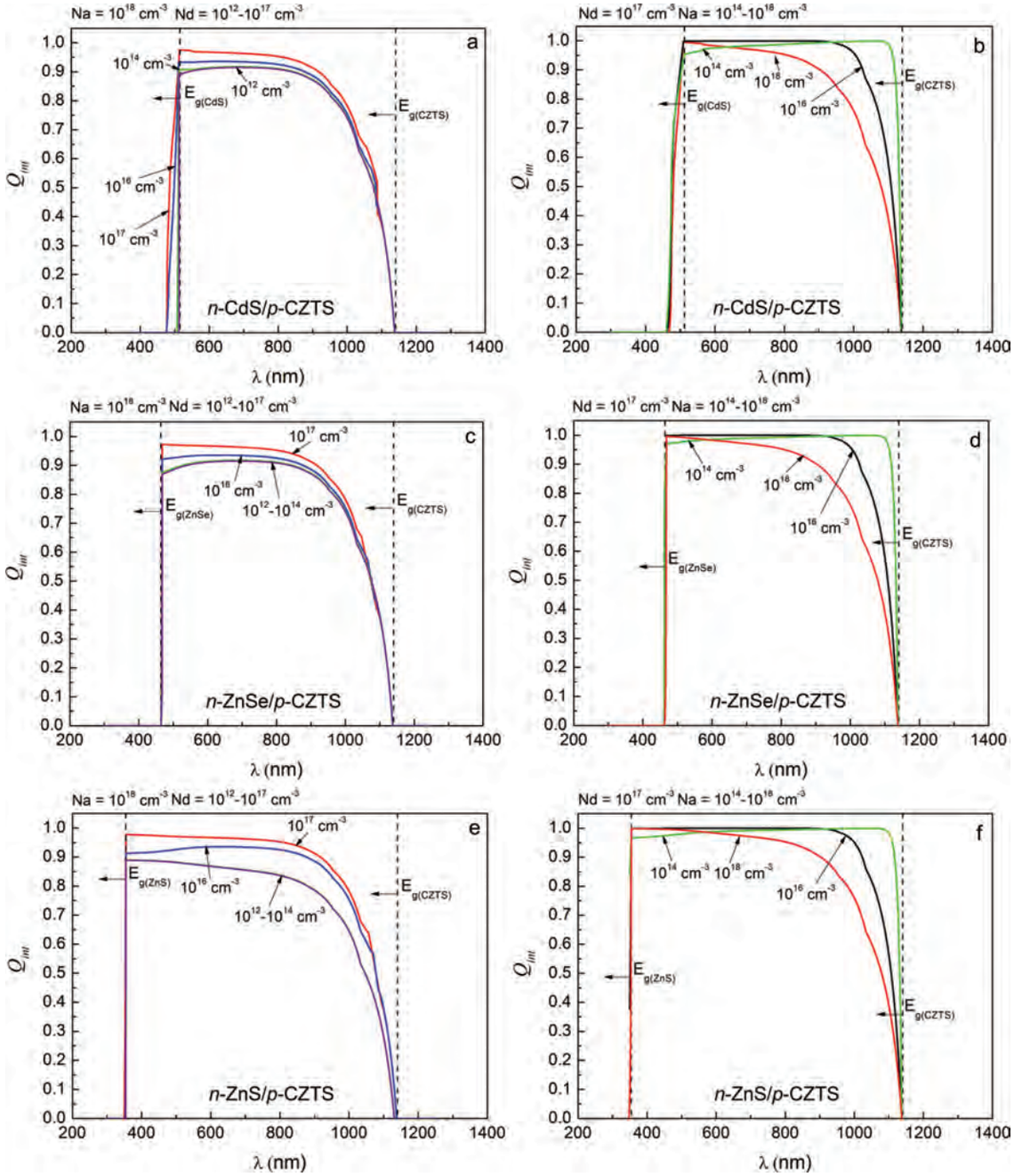

Fig. 7. Spectral dependencies of the internal quantum yields (Q_{int}) of the SCs based on *n*-CdS/*p*-CZTS (a, b), *n*-ZnSe/*p*-CZTS (c, d) and *n*-ZnS/*p*-CZTS (e, f) HJs with the different concentrations of $N_a = (10^{14}–10^{18})$ cm^{-3} and $N_d = (10^{12}–10^{17})$ cm^{-3}.

layer. To account these losses, the diffusion ($Q_{\text{dif}\,p(n)}$) component of the quantum yield can be evaluated by the following equation:[33]

$$
\begin{aligned}
&Q_{\text{dif}\,p(n)} \\
&\quad = ((\alpha_{p(n)}L_{np(pn)}/(\alpha^2_{p(n)}L^2_{np(pn)} - 1))\exp(-\alpha_{p(n)}w_{p(n)}) \\
&\qquad \times (\alpha_{p(n)}L_{np(pn)} - ((S_bL_{np(pn)}/D_{np(pn)}) \\
&\qquad \times (\cosh((d_{p(n)} - w_{p(n)})/L_{np(pn)}) - \exp(-\alpha_{p(n)}d_{p(n)} \\
&\qquad - w_{p(n)}))) + \sinh((d_{p(n)} - w_{p(n)})/L_{np(pn)}) \\
&\qquad + \alpha_{p(n)}L_{np(pn)}\exp((-\alpha_{p(n)}(d_{p(n)} - w_{p(n)})))) \\
&\qquad /((S_bL_{np(pn)}/D_{np(pn)})\sinh((d_{p(n)} - w_{p(n)})/L_{np(pn)}) \\
&\qquad + \cosh((d_{p(n)} - w_{p(n)})/L_{np(pn)})) \qquad (10)
\end{aligned}
$$

where $d_{p(n)}$—the thicknesses of the absorber and window layers; S_b—the recombination velocity in the quasineutral regions and on the back surface of the absorber layer.

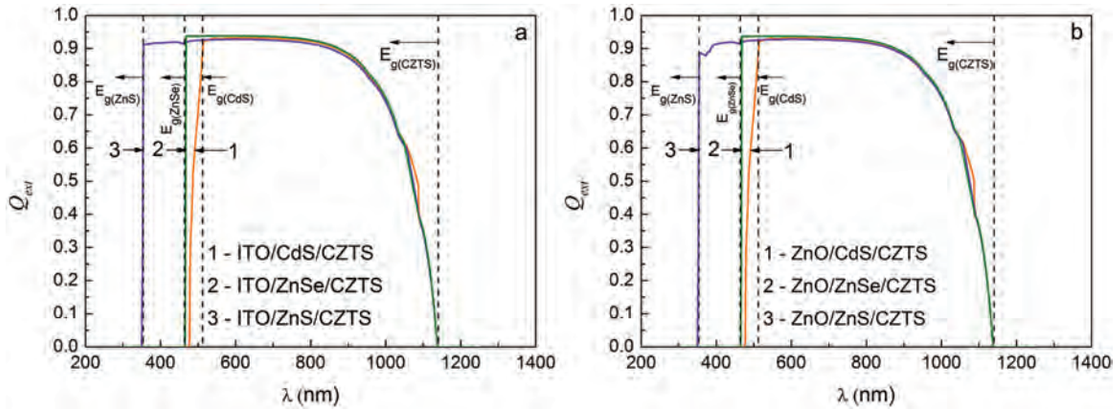

Fig. 8. Spectral dependencies of the external quantum yield (Q_{ext}) of the SCs based on *n*-CdS(ZnSe, ZnS)/*p*-CZTS HJs with ITO (a) and ZnO (b) charge-collecting layers with: $N_a = 10^{18}$ cm^{-3}, $N_d = 10^{17}$ cm^{-3}, $d_{ITO(ZnO)} = 100$ nm, $d_{CdS(ZnSe,ZnS)} = 25$ nm, $d_{CZTS} = 1$ μm.

The total internal quantum yield of the SCs is easy to determine as the sum of all quantum yields, considering the directions of the drift and diffusion currents in the space charge and quasineutral regions. The account of the optical losses owing to the reflection and absorption of the light by the auxiliary layers (ITO, CdS, ZnSe, ZnS) of the SCs gives the opportunity to determine the external quantum yield (Q_{ext}) of the device:[15]

$$Q_{ext} = T(\lambda)Q_{int} \tag{11}$$

The spectral dependencies of the internal quantum yields (Q_{int}) of the SCs with the different concentrations

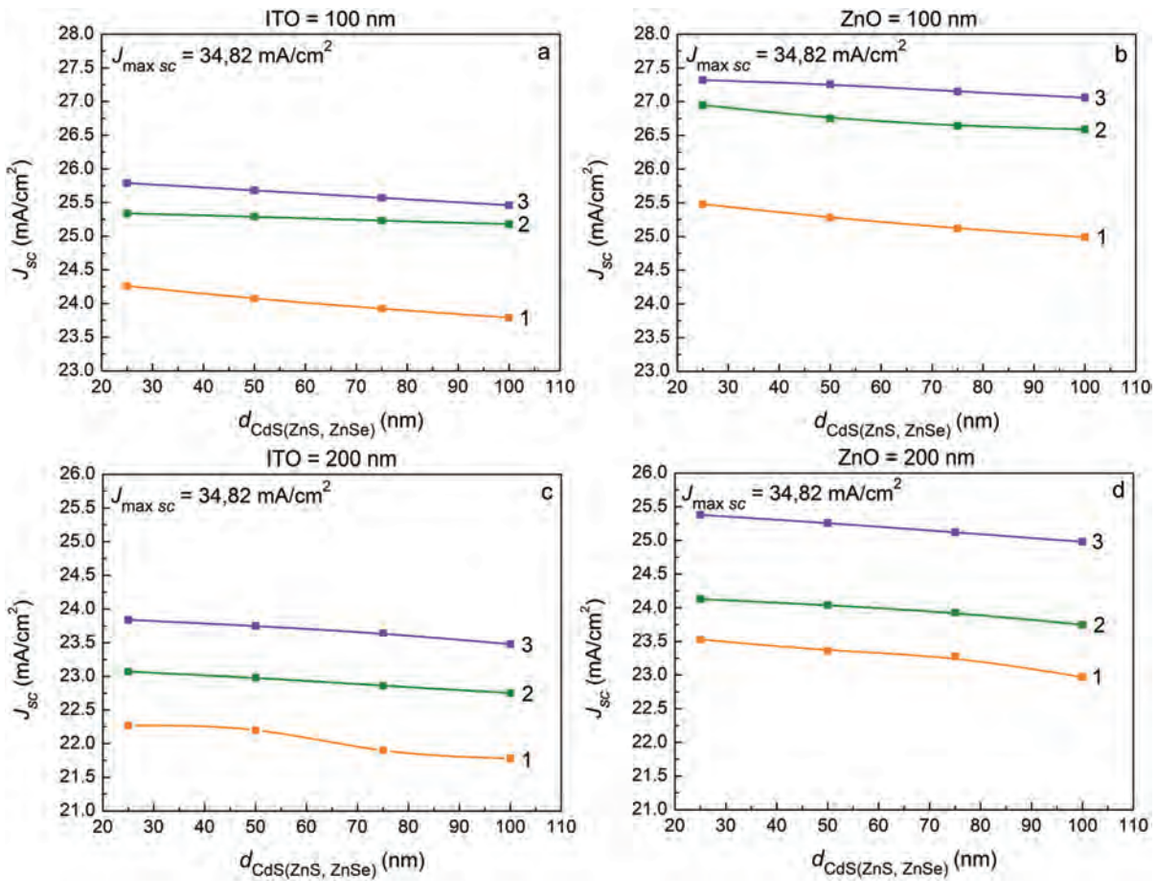

Fig. 9. Dependencies of the short-circuit current density (J_{sc}) on the window layer thicknesses of the SCs based on CdS/CZTS (1), ZnSe/CZTS (2), ZnS/CZTS (3) HJs with the charge-collecting layer thicknesses: 100 nm (a, b) and 200 nm (c, d).

of uncompensated acceptors (N_a) and donors (N_d) in the absorber and window layers are depicted in Figure 7. The calculations were performed for the SCs with the thicknesses of 1 μm of absorber layer ($A_{hv} = \sim 97\%$) and 25 nm of window layer (the minimum technologically reachable thickness of the window layer[52]).

It was established that the increase of the donor concentration in the window material (Fig. 7(a)) at the constant values of N_a in the absorber layer led to the increase in the quantum efficiency of the SC based on *n*-CdS/*p*-CZTS HJ in the photosensitive region for both CZTS and CdS materials. However, this increase had a weak influence on the internal quantum yield in the photosensitive region of the window materials in the SCs based on *n*-(ZnSe, ZnS)/*p*-CZTS HJs (Figs. 7(c, d)). This is understandable since ZnS and ZnSe absorb the solar spectrum weakly because of the wide band gaps of the materials. For the investigated HJs, the increase of the donor concentration caused the increase of the quantum yields in both middle and long wavelength regions, due to the extension of SCR in the absorber layer, and, as a consequence, reduced the impact of the diffusion component on the total photocurrent (J_{ph}).

Then, we investigated the effect of the alteration of the acceptor concentration on Q_{int} at the constants of the donor concentration (Figs. 7(b, d, f)). As can be seen from figures, the internal quantum yield is decreasing in the photosensitive regions of the absorber layer material that can be explained by the decreasing of the width of SCR due to the increasing of the diffusion component of the photocurrent. The optical losses described in the previous subsections are important for the analysis of the SC efficiency. As a consequence of its consideration, we built the spectral dependencies of the external quantum yield (Q_{ext}) for the investigated SCs. The calculations were carried out using the following physical values: $N_a = 10^{18}$ cm^{-3}, $N_d = 10^{17}$ cm^{-3}, $d_{ITO(ZnO)} =$ 100 nm, $d_{CdS(ZnSe,\,ZnS)} = 25$ nm, $d_{CZTS} = 1$ μm. The concentrations of uncompensated acceptors and donors coincide with SCR widths which are close to the device thicknesses. At the same time, the thicknesses of all functional layers were taken close to those used in the practical SCs.[5, 52]

The analysis of the obtained dependencies (Fig. 8) showed that the values of Q_{ext} of the SC based on *n*-ZnS/*p*-CZTS HJ are slightly higher than those of the structure with CdS and ZnSe window layers regardless of the

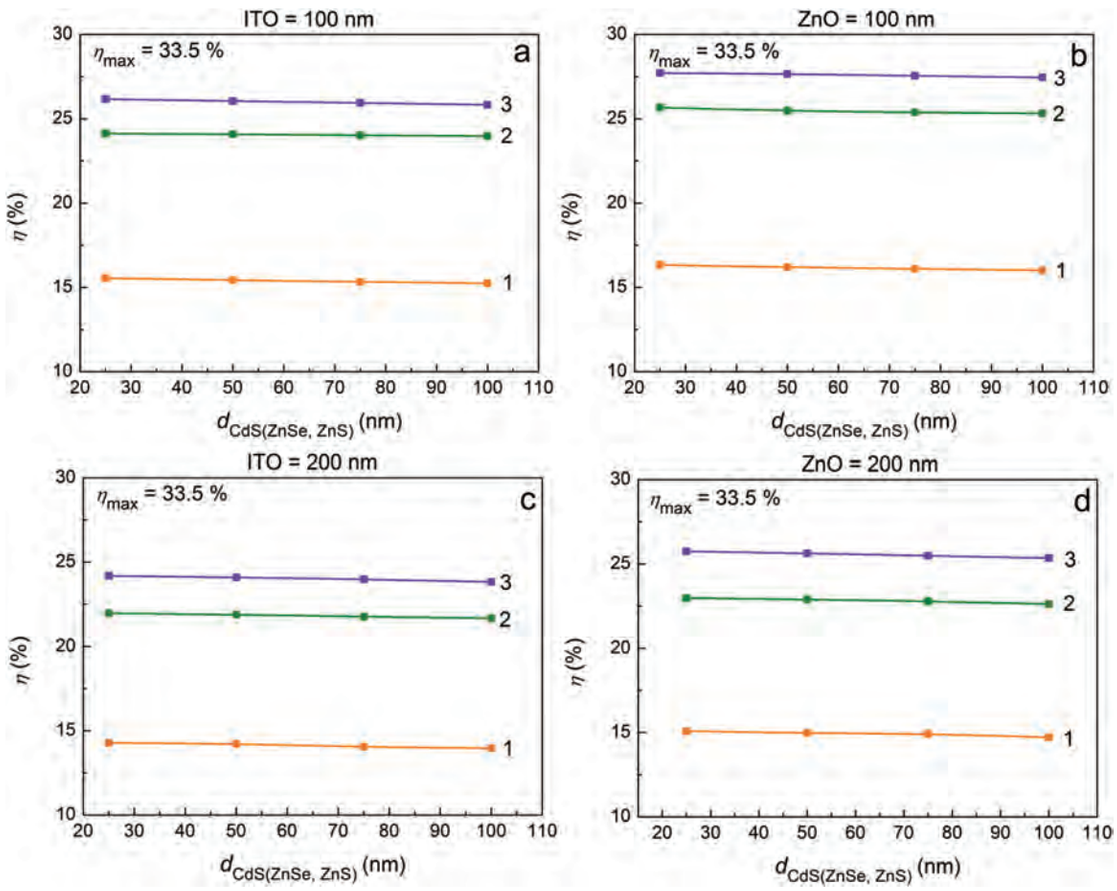

Fig. 10. The effect of the optical and recombination losses on the efficiency of the SCs based on CdS/CZTS (1), ZnSe/CZTS (2), ZnS/CZTS (3) HJs with the variable thicknesses of the window layers and two constant thicknesses of the charge-collecting contacts: 100 nm (a, b) and 200 nm (c, d).

material of the charge-collecting contacts. Thus, as it was expected, SCs with the window layers, which possess the higher values of the band gap, demonstrate the higher quantum yields.

However, it should be noted that we neglected the inequality state at the interfaces of the different HJs. However, in reality, the mismatch density of the dislocations at the interfaces of the considered HJs is varied.

3.2. The Determination of the Short-Circuit Current Density (J_{sc}) of the SCs

The short-circuit current density (J_{sc}) of the SCs was determined using the well-known formula:

$$J_{sc} = q\sum_i T(\lambda)\frac{\Phi_i(\lambda_i)}{hv_i}Q_{int}(\lambda_i)\Delta\lambda_i \quad (12)$$

where $\Phi_i(\lambda_i)$—the spectral power density of the solar radiation; $\Delta\lambda_i$—the interval between neighboring values of the wavelength; hv_i—the photon energy.

The calculation of J_{sc} was carried out under AM 1.5G radiation conditions.[53] Herewith, the maximum short-circuit current density ($J_{max\,sc}$) can be obtained by neglecting the light losses owing to the absorption of the auxiliary layers, i.e., $T(\lambda) = 1$, and under the circumstance that every photon generates the electron–hole pair which reaches the charge-collecting contacts without recombination, i.e., $Q_{ext}(\lambda) = 1$. It was established, that the maximum value of the short-circuit current density of the investigated SCs is equaled to $J_{max\,sc} = 34.82$ mA/cm^2. This result correlates well with the obtained one in Ref. [5] for SCs based on the materials with the close band gap to the considered semiconductors. However, from the practical point of view, this result is not achievable due to the losses occurring during the photoelectric conversion of the solar energy.

The dependencies of the short-circuit current density (J_{sc}) of ITO(ZnO)/CdS(ZnSe, ZnS)/CZTS SCs on the thicknesses of the window layer considering the optical and recombination losses in the auxiliary layers are shown in Figure 10. It was assumed that the thicknesses of ITO (ZnO) charge-collecting layers were 100 nm and 200 nm. The obtained values of J_{sc} are presented in Table VI.

It was found that, under the consideration of the losses owing to the reflection and absorption of the auxiliary layers, the values of J_{sc} of the SCs with ZnO/ZnS/CZTS ($d_{ZnS} = (25–100)$ nm, $d_{ITO(ZnO)} = 100$ nm) structure were higher in (3.06–3.27) mA/cm^2 than those obtained for the devices with ITO/CdS/CZTS structure in the overall interval of the thickness alteration. The increase of the charge-collecting layer thickness up to 200 nm resulted in the decrease of J_{sc} and the difference between the best (ZnO/ZnS/CZTS) and worst (ITO/CdS/CZTS) structures was found to be ~3.15 mA/cm^2. It should be noted that the optical and recombination losses led to the decrease of J_{sc} by (21.5–37.4)%.

Table VI. The values of the short-circuit current density (J_{sc}, mA/cm^2) of the SCs with ITO(ZnO)/CdS(ZnSe, ZnS)/CZTS structures.

No.	Thin film solar cell structure	Window layer thickness			
		$d_{ITO(ZnO)} = 100$ nm			
	$d_{CdS(Zne,\,ZnS)}$, nm	25	50	75	100
1	ZnO/ZnS/CZTS	27.32	27.26	27.15	27.06
2	ZnO/ZnSe/CZTS	26.95	26.75	26.64	26.59
3	ZnO/CdS/CZTS	25.48	25.28	25.12	24.99
4	ITO/ZnS/CZTS	25.79	25.68	25.57	25.46
5	ITO/ZnSe/CZTS	25.34	25.29	25.23	25.18
6	ITO/CdS/CZTS	24.26	24.07	23.92	23.79
		$d_{ITO(ZnO)} = 200$ nm			
1	ZnO/ZnS/CZTS	25.38	25.26	25.12	24.98
2	ZnO/ZnSe/CZTS	24.13	24.04	23.93	23.75
3	ZnO/CdS/CZTS	23.53	23.36	23.28	22.97
4	ITO/ZnS/CZTS	23.84	23.75	23.64	23.48
5	ITO/ZnSe/CZTS	23.07	22.98	22.86	22.75
6	ITO/CdS/CZTS	22.27	22.20	21.90	21.78

4. THE EFFECT OF RECOMBINATION AND OPTICAL LOSSES ON THE MAXIMUM EFFICIENCY OF THE SOLAR CELLS

The solar cell efficiency (η) is determined by the well-known equation:[10, 29, 38]

$$\eta = \frac{U_{oc}\cdot J_{sc}\cdot FF}{P_{in}} \quad (13)$$

where U_{oc}—the open-circuit voltage; J_{sc}—the short-circuit current density; FF—the fill factor; P_{in}—the input power (100 mW/cm^2, illumination AM 1.5G).

To determine the effect of the optical and recombination losses on the maximum efficiencies of the SCs with ITO(ZnO)/CdS(ZnSe, ZnS)/CZTS structures, the values of open-circuit voltage were taken as those that coinciding with the height of the contact potential differences at the HJs: $U_{oc} = (0.72\text{ V})_{CdS}$, $(1.07\text{ V})_{ZnSe}$, $(1.14\text{ V})_{ZnS}$, and the values of the fill factor that matching the maximum possible $FF = 89\%$.[5] Accordingly, it was found that the maximum efficiency of the single junction SC was 33.5%.[5]

The dependencies of the SC efficiencies (η) on the thicknesses of the window (CdS, ZnSe, ZnS) and charge-collecting (ITO, ZnO) layers are presented in Figure 10. As can be seen from Figure 10, the best devices, among the investigated SC structures, contain ZnS window layer ($\eta = 23.8–27.7\%$), and the highest values of the efficiency were demonstrated by a device with ZnO/ZnS/CZTS structure ($\eta \sim 28\%$ with $d_{ZnO} = 100$ nm, $d_{ZnS} = 25$ nm).

It should be mentioned, that the efficiency of the well-known SC with ITO/CdS/CZTS structure was about (13.9–15.5)%. These values are well correlated with the results obtained for the best SC with the analogous structure ($\eta = 12.6\%$).[11, 12] The SCs with ZnSe window layer showed the quite high efficiencies as well, $\eta = (21.7–25.7)\%$.

5. CONCLUSIONS

In this work, the optical and recombination losses in the SCs based on *n*-CdS/*p*-CZTS, *n*-ZnSe/*p*-CZTS, *n*-ZnS/*p*-CZTS HJs with ITO (ZnO) frontal charge-collecting contacts were investigated. The effect of these losses on the internal (Q_{int}), external (Q_{ext}) quantum yields, short-circuit current density (J_{sc}) and maximum efficiency (η) of the SCs was studied.

The analysis of the optical losses owing the light reflection and absorption of the window and charge-collecting layers showed that, as it was expected, the replacement of the traditional window material (CdS) with wide band gap materials (ZnSe, ZnS) caused the increase of the transmission coefficients of the multilayer structures, primarily, in the short wave region with $d_{CdS(ZnSe,\,ZnS)} = (25–100)$ nm. This tendency was valid for applying ITO and ZnO layers with $d_{ITO(ZnO)} = (100–200)$ nm as the charge-collecting contacts.

ZnO layer is more attractive than ITO because it improves the light transmission coefficients toward CZTS absorber layer regardless of the considered window materials.

To determine the recombination losses in the SCs, we have built the energy band diagrams of *n*-CdS(ZnSe, ZnS)/*p*-CZTS HJs.

It was established that the increase of the donor concentration in the window material at the constant values of N_a in the absorber layer resulted in the increase of the quantum efficiency of the SC based on *n*-CdS/*p*-CZTS HJ in the photosensitive region for both CZTS and CdS materials. However, this increase had a weak influence on the internal quantum yield in the photosensitive region of the window materials in the SCs based on *n*-(ZnSe, ZnS)/*p*-CZTS HJs. For the investigated HJs, the increase of the donor concentration caused the increase of the quantum yields in both middle and long wavelength regions, due to the extension of SCR in the absorber layer, and, as a consequence, reduced impact of the diffusion component on the total photocurrent (J_{ph}).

The analysis of the obtained dependencies showed that the values of Q_{ext} of the SC based on *n*-ZnS/*p*-CZTS HJ were slightly higher than those of the structure with CdS and ZnSe window layers regardless of the material of the charge-collecting contacts. Thus, as it was expected, SCs with the window layers, which possess the higher values of the band gap, demonstrated the higher quantum yields.

It was found that, under the consideration of the losses owing to the reflection and absorption of the auxiliary layers of devices, the values of J_{sc} of the SCs with the ZnO/ZnS/CZTS ($d_{ZnS} = (25–100)$ nm, $d_{ITO(ZnO)} = 100$ nm) structure were higher in (3.06–3.27) mA/cm^2 than those obtained for devices with ITO/CdS/CZTS structure in the overall interval of the thickness alteration. The increase of the charge-collecting layer thickness up to 200 nm led to the decrease of J_{sc} and the difference between the best (ZnO/ZnS/CZTS) and worst (ITO/ZnSe/CZTS) structures of the SCs was found to be ~3.15 mA/cm^2. It should be noted that the optical and recombination losses caused the decrease of J_{sc} by (21.5–37.4)%.

The best devices, among the investigated SC structures, contain ZnS window layer ($\eta = 23.8–27.7\%$), and the highest values of the efficiency were demonstrated by the device with ZnO/ZnS/CZTS structure (η~28% with $d_{ZnO} = 100$ nm, $d_{ZnS} = 25$ nm). The SCs with ZnSe window layer showed the quite high efficiency as well, $\eta = (21.7–25.7)\%$. It should be mentioned, that the efficiency of the well-known SC with ITO/CdS/CZTS structure was about (13.9–15.5)%. These values are well correlated with the results obtained for the best SC with the analogous structure ($\eta = 12.6\%$).

The presented results show the maximum values of the efficiencies of the SCs based on *n*-CdS(ZnSe, ZnSe)/*p*-CZTS HJs and open the way for the optimization of the practical thin film SCs.

Acknowledgments: This work was supported by the Ministry of the Education and Science of Ukraine (Grant numbers 0116U002619, 0115U000665c, 0116U006813).

References and Notes

1. N. Kannan and D. Vakeesan, *Renewable Sustainable Energy Rev.* 62, 1092 **(2016)**.
2. S. M. Sze and K. K. Ng, Physics of Semiconductor Devices, John Wiley & Sons, Hoboken **(2006)**.
3. http://investor.firstsolar.com/releasedetail.cfm?ReleaseID=956479.
4. S. Girish Kumar and K. S. R. Koteswara Rao, *Energy Environ. Sci.* 7, 45 **(2014)**.
5. K. Ito, Copper Zinc Tin Sulfide-Based Thin Film Solar Cells, John Wiley & Sons, Chichester **(2015)**.
6. M. P. Suryawanshi, G. L. Agawane, S. M. Bhosale, S. W. Shin, P. S. Patil, J. H. Kim, and A. V. Moholkar, *Mater. Technol.* 28, 98 **(2013)**.
7. M. Nguyen, K. Ernits, K. F. Tai, C. F. Ng, S. S. Pramana, W. A. Sasangka, S. K. Batabyal, T. Holopainen, D. Meissner, and A. Neisser, *Sol. Energy* 111, 344 **(2015)**.
8. H. Katagiri, K. Saitoh, T. Washio, H. Shinohara, T. Kurumadani, and S. Miyajima, *Sol. Energy Mater. Sol. Cells* 65, 141 **(2001)**.
9. O. Dobrozhan, A. Opanasyuk, M. Kolesnyk, M. Demydenko, and H. Cheong, *Phys. Status Solidi A* 212, 2915 **(2015)**.
10. A. Polman, M. Knight, E. C. Garnett, B. Ehrler, and W. C. Sinke, *Challenges Science* 352, aad4424 **(2016)**.
11. W. Wang, M. T. Winkler, O. Gunawan, T. Gokmen, T. K. Todorov, Y. Zhu, and D. B. Mitzi, *Adv. Energy Mater.* 4, 1301465 **(2014)**.
12. M. A. Green, K. Emery, Y. Hishikawa, W. Warta, and E. D. Dunlop, *Prog. Photovoltaics* 24, 905 **(2016)**.
13. M. Houshmand, M. H. Zandi, and N. E. Gorji, *Mater. Lett.* 164, 493 **(2016)**.
14. L. A. Kosyachenko, X. Mathew, P. D. Paulson, V. Ya. Lytvynenko, and O. L. Maslyanchuk, *Sol. Energy Mater. Sol. Cells* 130, 291 **(2014)**.
15. L. A. Kosyachenko, V. Y. Lytvynenko, and O. L. Maslyanchuk, *Semiconductors* 50, 508 **(2016)**.

16. T. Mykytyuk, V. Y. Roshko, L. Kosyachenko, and E. Grushko, *Acta Phys. Pol. A* 122, 1073 **(2012)**.
17. L. A. Kosyachenko, X. Mathew, V. Y. Roshko, and E. V. Grushko, *Sol. Energy Mater. Sol. Cells* 114, 179 **(2013)**.
18. O. A. Dobrozhan, T. O. Berestok, D. I. Kurbatov, A. S. Opanasyuk, N. M. Opanasyuk, and V. F. Nefedchenko, Optical losses of thin solar cells on the basis of n-ZnS/p-CdTe and n-CdS/p-CdTe heterojunctions, *Proceedings of the 3rd International Conference Nanomaterials: Applications and Properties*, Alushta, Ukraine, September **(2013)**.
19. O. A. Dobrozhan, A. S. Opanasyuk, and V. F. Nefedchenko, Recombination losses in solar cells based on n-ZnS(n-CdS)/p-CdTe heterojunctions, *Proceedings of the 4th International Conference Nanomaterials: Applications and Properties*, Alushta, Ukraine, September **(2014)**.
20. L. A. Kosyachenko, E. V. Grushko, and X. Mathew, *Sol. Energy Mater. Sol. Cells* 96, 231 **(2012)**.
21. L. A. Kosyachenko, *Mater. Renewable Sustainable Energy* 2, 14 **(2013)**.
22. H. A. Mohamed, *Can. J. Phys.* 92, 1350 **(2014)**.
23. M. Aldosari, H. Sohrabpoor, and N. E. Gorji, *Superlattices Microstruct.* 92, 242 **(2016)**.
24. O. Dobrozhan, A. Opanasyuk, and V. Grynenko, *J. Nano-Electron. Phys.* 6, 04035 **(2014)**.
25. L. A. Kosyachenko, E. V. Grushko, and V. V. Motushchuk, *Sol. Energy Mater. Sol. Cells* 90, 2201 **(2006)**.
26. M. Houshmand, M. H. Zandi, and N. E. Gorji, *Superlattices Microstruct.* 97, 424 **(2016)**.
27. N. E. Gorji, *IEEE Trans. Nanotechnol.* 13, 743 **(2014)**.
28. H. A. Mohamed, *J. Appl. Phys.* 113, 093105 **(2013)**.
29. S. O. Kasap, Optoelectronics and Photonics: Principles and Practices, Prentice Hall, Upper Saddle River **(2001)**.
30. S. Adachi (ed.), Handbook on Physical Properties of Semiconductors, Kluwer Academic Publishers, Berlin **(2004)**.
31. http://refractiveindex.info/?shelf=main&book=ZnSe&page=Connolly.
32. A. S. Opanasyuk, D. I. Kurbatov, M. M. Ivashchenko, I. Yu. Protsenko, and H. Cheong, *J. Nano-Electron. Phys.* 4, 01024 **(2012)**.
33. L. Kosyachenko and T. Toyama, *Sol. Energy Mater. Sol. Cells* 120, 512 **(2014)**.
34. L. A. Kosyachenko, *Semiconductors* 40, 710 **(2006)**.
35. D. Kurbatov, V. Kosyak, A. Opanasyuk, and V. Melnik, *Phys. B* 404, 5002 **(2009)**.
36. S. J. Pearton, Processing of Wide Band Gap Semiconductors, Cambridge University Press, Cambridge **(2000)**.
37. O. Madelung, U. Rossler, and W. Von der Osten, Intrinsic Properties of Group IV Elements and III–V, II–VI and I–VII Compounds, Springer-Verlag, Berlin, Heidelberg **(1987)**.
38. H. Flammersberger, Experimental Study of Cu_2ZnSnS_4 Thin Films for Solar Cells, Ph.D. Thesis, Uppsala University **(2010)**, p. 117.
39. C. Shiyou, A. Walsh, X.-G. Gong, and S.-H. Wei, *Adv. Mater.* 25, 1522 **(2013)**.
40. M. Neuberger, Cadmium Sulfide: Summary Review and Data Sheets, Electronic Properties Information Center at Hughes Aircraft Company **(1963)**.
41. D. B. Laks, C. G. Van de Walle, G. F. Neumark, P. E. Blöchl, and S. T. Pantelides, *Phys. Rev. B* 45, 10965 **(1992)**.
42. I. P. Kalinkin and V. B. Aleskovskiy, Epitaksialnue Plenki Soedineniy A_2B_6, LGU, Leningrad **(1978)**, In russian.
43. A. V. Simashkevich, Heteroperehody Na Osnove Polyprovodnikovyh Soedineniy A_2B_6, Shtiinca, Kishinev **(1980)**, In russian.
44. N. K. Morozova and N. D. Danilevich, *Semiconductors* 44, 458 **(2010)**.
45. J. P. Teixeira, R. A. Sousa, M. G. Sousa, A. F. da Cunha, P. A. Fernandes, P. M. P. Salomé, and J. P. Leitão, *Phys. Rev. B* 90, 235202 **(2014)**.
46. R. D. Gould, Handbook of Thin Films, edited by H. S. Nalwa, Academic Press, Burlington **(2002)**, Chap. 4, pp. 187–245.
47. M. Balkanski and R. F. Wallis, Semiconductor Physics and Applications, Oxford University Press, Oxford **(2000)**.
48. W. B. Leigh, P. Besomi, and B. W. Wessels, *J. Appl. Phys.* 53, 532 **(1982)**.
49. C. G. Rodrigues, *Microelectron. J.* 37, 657 **(2006)**.
50. W. E. Spear and J. Mort, *Proc. Phys. Soc.* 81, 130 **(1963)**.
51. N. G. Basov (ed.), Exciton and Domain Luminescence of Semiconductors, Consultants Bureau, New York **(1979)**.
52. R. Scheer and H. W. Schock, Chalcogenide Photovoltaics: Physics, Technologies, and Thin Film Devices, Wiley-VCH Verlag GmbH & Co. KGaA, Weinheim **(2011)**.
53. Reference Solar Spectral Irradiance at the Ground at Different Receiving Conditions, Part 1: Direct Normal and Hemispherical Solar Irradiance for Air Mass 1.5, Standard of International Organization for Standardization, ISO 9845-1 **(1992)**.